

Modelling of degradation/recovery phenomena in CdS/CdTe ultrathin film solar cells

Nima E. Gorji

Received: 21 October 2014 / Accepted: 17 December 2014 / Published online: 27 December 2014
© Springer-Verlag Berlin Heidelberg 2014

Abstract The degradation/recovery phenomena in ultrathin film solar cells based on CdS/CdTe are theoretically analysed using Sah–Noyce–Shockley theory for generation and recombination in the depletion region. This theory can explain the overlap of the depletion regions at both front and back contacts where the carrier generation and collection are as important as recombination mechanism. The value of physical parameters such as uncompensated defect density, carrier recombination lifetime and band bending at interface are critically important when reducing the thickness of CdTe layer down to sub-micron. The rollover, materials inter-/out-diffusion, complex defect formation and the role of mobile ions are taken into consideration to obtain an insight into the physics of degradation/recovery phenomena in ultrathin CdTe film solar cells. Both mechanisms are precisely analysed drawing the schematics of the energy band diagrams and mobile ions transport paths which in this case is the grain interior. This means that we neglect the metal diffusion through the grain boundaries which are assumed to be completely passivated. This assumption enabled us to study the role of the defects on the carrier transport in the interiors rather than through the boundaries.

1 Introduction

So far, just a few theoretical analysis have been performed on the carrier transport and charge collection in ultrathin CdS/CdTe film solar cells ($d \leq 1 \mu\text{m}$) taking into account

the carrier generation and collection in both depletion regions at space charge region (SCR) and back contact (BC). The thickness of such devices (d) is comparable with the width of SCR (W) and carrier diffusion length (L_n). Karpov et al. [1] have studied the unique physics of ultrathin photovoltaics (PV) by assuming $W > d$. They considered that an ultrathin device resembles a capacitance with a dielectric inside it. In another approach, Kosyachenko and Toyama [2] have analysed the thin-film devices with $d = 2.7 \mu\text{m}$ and showed that the influence of BC on the carrier transport in SCR can be ignored if the concentration of uncompensated acceptors, $N_{ad} = 5 \times 10^{15} \text{cm}^{-3}$, and the depletion widths of SCR ($W = 0.6\text{--}0.8 \mu\text{m}$) do not overlap with the depletion width of the BC ($W_b = 0.2 \mu\text{m}$). In fact, band bending at the BC is smaller than in junction (CdS/CdTe), and hence, its depletion layer is narrower. This allows considering a flat energy band outside of SCR (from W to BC). The latter assumption is also possible about the ultrathin films where W and d are comparable. The widths of the depletion layers become important in stabilization/degradation/recovery issues of CdTe devices under different operation conditions. For example, several research groups have confirmed that the dark resting of open-circuited device can slightly recover the performance [3, 4]. The quantum efficiency measurements of ultrathin devices fabricated by Paudel et al. have indicated that forward bias (0.4–0.5 V) can reduce the carrier collection by lowering the electric field in SCR. In contrary, the reverse-biased devices have enhanced the quantum efficiency due to faster current collection by extended electric field to BC and preventing the carrier recombination there [5]. The performance of the thinner devices ($W < 0.5 \mu\text{m}$) showed a stronger dependency on applied bias representing the importance of SCR width for $d < 1 \mu\text{m}$.

N. E. Gorji (✉)
Department of Electrical, Electronic, and Information
Engineering, University of Bologna, 40136 Bologna, Italy
e-mail: nima.eshaghgorji2@unibo.it

The reduced depletion width in the ultrathin films can lead to increased recombination rate at CdTe/metal. While the low performance of ultrathin devices is mostly due to incomplete photo-absorption, the degradation and recovery of the electrical parameters is related to the electric field variation. The resultant of the electric fields, across the CdTe layer, can alter the carrier transport via defects inter/back-diffusion into CdTe or BC.

In this study, we will take into account the role of carrier collection in ultrathin devices rather than incomplete photo-absorption which can clearly reduce the short-circuit current and efficiency [3]. We will simulate the degradation/recovery phenomena in CdTe devices after degradation under accelerated life testing (ALT) or recovery under dark storage. It was observed that the devices left in dark rest and/or under illumination while short and/or open circuited could be partially or completely recovered [3, 4]. We will also study the variation of depletion width by defect density and voltage as well as the effects of physical parameters on the characteristics of ultrathin devices under forward or reverse biases. The interesting conclusion of such analysis is that the degradation of thin-film devices is not always permanent (irreversible) but rather can be (slightly) recovered under a proper bias (i.e. short circuit) and illumination and/or re-annealing. The recovery was suggested to be due to change in the concentration of defect density or mobile ions (Cu^+) that diffuse back to the BC and reduce the recombination centres at the SCR (junction) [6]. We note here that our approach is not modelling the inter-diffusion of the Cu ions through grain boundaries, but we assume that the grains size ($\geq 1 \mu\text{m}$) is as big as the CdTe layer and the defective particles are diffusing through bulk CdTe. This approach can be extended to the other type of materials such as radiation detectors based on CdTe and CdZnTe as well as thin-film solar cells based on CIGS and CZTS materials [6–8]. Further investigations are required for the realization of durable and stable semi-transparent PV windows using ultrathin films proposed and practically introduced by Plotnikov et al. [9].

2 Theory

For the modelling of the recombination–generation mechanism in thin-film solar cells based on CIGS materials, we have had proposed a simple approach for the carrier transport in the different regions of the absorber layer separately [10]. Current study will analyse a more comprehensive approach where the most practically known parameters of the device are taken into consideration.

As shown in Fig. 1, the formation of SCR at the interface of a thin-film CdS/CdTe is similar to the formation of a depletion region at the p–n junction of a Schottky diode.

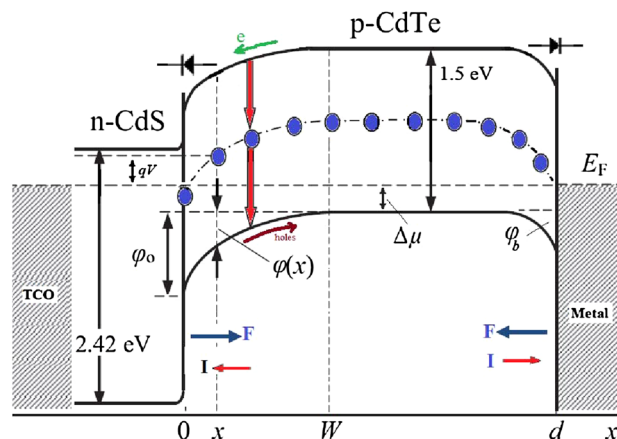


Fig. 1 The energy band diagram of CdS/CdTe thin film under forward bias. The carrier transport through recombination–generation (I_{gr}) and over-barrier current (I_n), SCR (W), band bending strength $\varphi(x)$ and Fermi levels are indicated

Since the CdS layer is well conductive, the SCR width of the solar cell is considered to be only in the CdTe p-type layer given by,

$$W = \sqrt{\frac{2\varepsilon(\varphi_0 - qV)}{q^2(N_a - N_d)}} \quad (1)$$

where ε is the relative permittivity of the semiconductor, $\varphi_0 = qV_{bi}$ is the barrier height at the semiconductor side (V_{bi} is built-in potential), q is the electron charge, V is the applied voltage and $N_a - N_d = N_{ad}$ is the concentration of uncompensated acceptors in the CdTe layer. The non-uniform electric field strength for electrons in SCR at the distance x from the interface depends on W via,

$$F(x) = \frac{(\varphi_0 - qV)}{qW} \left(2 - \frac{x}{W}\right) \rightarrow \bar{F} = \frac{2(\varphi_0 - qV)}{W} \quad (2)$$

and band bending in SCR is described by the parabolic law [11],

$$\varphi(x, V) = (\varphi_0 - qV) \left(1 - \frac{x}{W}\right)^2. \quad (3)$$

The current density–voltage (JV) characteristics of the thin-film solar cell can be considered using Sah–Noyce–Shockley theory for the generation–recombination under reverse–forward biases [12, 13]. The forward and reverse currents are quite sensitive to the position of the defects in the band gap. For example, if the generation–recombination level situated in the upper part of the band gap ($E > E_g/2$ with $E_g = 1.5 \text{ eV}$), with a distance more than 0.25 eV away from the midgap, the voltage dependence of the forward current is given by Eq. 4. In a same way, if the defect level was in the lower part of the midgap with a distance more than -0.25 eV , the forward current can be given by Eq. 5 [13],

$$J_{\text{forw}} = \frac{qp_1W}{\tau_{\text{po}}} \frac{\sqrt{E_g - 2\Delta\mu - qV} - \sqrt{E_t - qV}}{\sqrt{\varphi_0 - qV}} \exp\left(\frac{qV}{kT}\right),$$

if $E > E_g/2$ (4)

$$J_{\text{forw}} = \frac{qn_1W}{\tau_{\text{no}}} \frac{\sqrt{E_t - \Delta\mu - qV} - \sqrt{E_g - E_t - \Delta\mu}}{\sqrt{\varphi_0 - qV}} \exp\left(\frac{qV}{kT}\right),$$

if $E < E_g/2$ (5)

On the other hand, the current of the reverse bias for the case $E > E_g/2$ and $E < E_g/2$ is given, respectively, as,

$$J_{\text{rev}} = \frac{qp_1W}{\tau_{\text{po}}} \frac{\sqrt{E_g - \Delta\mu - E_t - qV} - \sqrt{E_t - qV}}{\sqrt{\varphi_0 - qV}},$$

if $E > E_g/2$ (6)

$$J_{\text{rev}} = \frac{qn_1W}{\tau_{\text{no}}} \frac{\sqrt{E_t - \Delta\mu - qV} - \sqrt{E_g - E_t - \Delta\mu}}{\sqrt{\varphi_0 - qV}},$$

if $E < E_g/2$ (7)

The values n_1 and p_1 are determined by the following equations with the energy spacing between the top of the valence band and Shockley–Read–Hall recombination level, E_t ,

$$n_1 = N_c \exp\left(-\frac{E_g - E_t}{kT}\right), \quad p_1 = N_v \exp\left(-\frac{E_t}{kT}\right). \quad (8)$$

Note that the above formulas are obtained assuming $|qV| \gg kT$. In Ref. [13], the diffusion model (rather than the diode model) was suggested for the carrier transport at high forward biases. The above equations come from the integration over SCR of the generation–recombination equation $[U(x,V)]$ of Sah–Noyce–Shockley theory when $V < 0.8$ V [12]. The above equations are separated functions from the main equation of the current density ($J = q_0 \int U(x,V) dx$) which is the product of the integrand’s maximum value and its half width. Note that this theory considers the carrier transport in the SCR only. At the BC of the device, where a reverse diode is formed (Fig. 2), the JV curves show a rollover which is ascribed to Schottky barrier. The depth of this barrier depends on the CdTe thickness as well as on the employed BC metal. The simulation results of Hadrich et al. [14] show that the back barrier is removed for the ultrathin devices with $d \leq 1$ μm . The ultrathin devices have sufficiently large SCR width, W , at CdS/CdTe that will overcome (overlap) the back depletion width, W_b (back barrier). This will diminish the rollover in JV curve of the device as the back barrier is no longer influent on the carrier transport at the BC. Nevertheless, we would like to also bring the equation that calculates the current at the BC. Kosyachenko et al. [13] have tried to make a modelling for rollover mechanism using the well-known thermionic emission theory where the current density is given by,

$$J_{\text{th}} = qA^* \exp\left(-\frac{\varphi_0 + \Delta\mu}{kT}\right) \left[\exp\left(\frac{qV}{kT}\right) - 1\right] \quad (9)$$

where A_* is the effective Richardson constant. However, there are some discrepancies between the experimental data and Eq. (9) for the bias range of $V > 0.2$ V. This disagreement comes from the fact that the above equation is applicable to the case that the diffusion length of the electrons is bigger than the depletion width. When $L_n \approx 1$ μm and $W = 0.8$ – 1 μm , the above formulation need to be revised. Thus, they suggested that the diffusion model can better fit the conditions and define the carrier transport in the back region. Therefore, the diffusion current of Eq. (9) is replaced by the form,

$$J_{\text{diff}} = q\mu_n \frac{2(\varphi_0 - qV)}{qW} N_c \exp\left(-\frac{\varphi_0 + \Delta\mu}{kT}\right) \left[\exp\left(\frac{qV}{kT}\right) - 1\right] \quad (10)$$

where the electron concentration at the semiconductor surface (rather than in the bulk of the film) is described by,

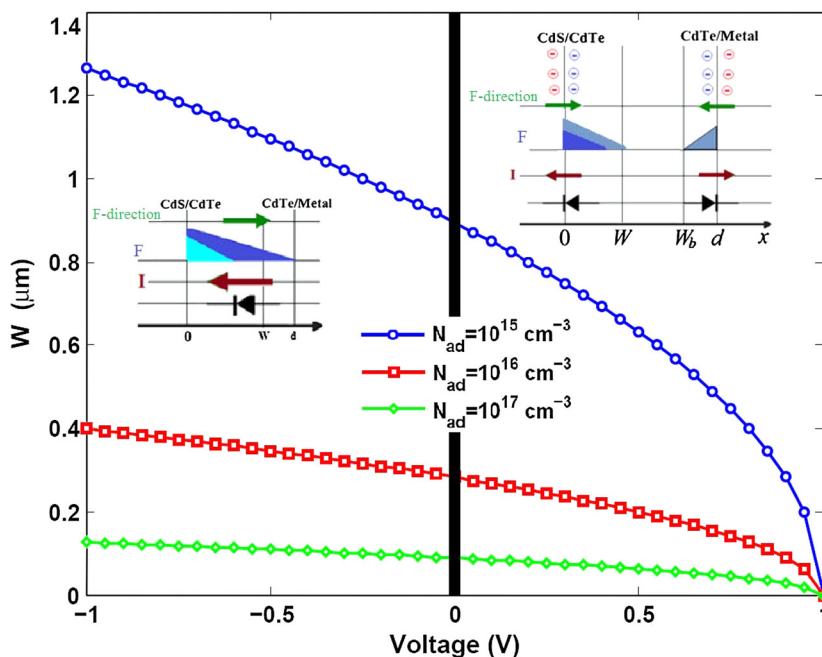
$$n = N_c \exp\left[-\frac{E_g - \Delta\mu - \varphi(x,V) - qV}{kT}\right] \quad (11)$$

Note that the first term (pre-exponential factor) in Eq. (10) depends on the applied bias while in Eq. (9), qA^* is voltage independent. The last equation will be able to explain the observed rollover in the JV curves of the solar cell regarding the BC issues. The same dependency on the voltage was reported in Ref. [14]. In case that our simulations were not consistent with the literature reports, the Eqs. (9) and (10) are taken into consideration.

3 Simulation results and discussion

Based on the theory of the last section, the variation of depletion width (SCR) versus voltage has been calculated for different uncompensated defect densities (Fig. 2). Higher density of uncompensated defects, N_{ad} , can narrow the depletion width, whereas the reverse and forward biases have a different influences. The insets give a schematic view on the strength of electric field in the reverse and forward bias regions and flow direction of the carrier current in each SCR and BC regions. The distribution of charge carriers, electric fields, current and relevant diodes under open-circuit condition is indicated for a better understanding. At the BC region, there is a small charge distribution that can be simulated as a Schottky barrier with an opposite diode. This barrier can cause rollover in the high forward bias range of the JV curves. The reverse bias extends the electric fields across the CdTe layer corresponding to a single diode model. On the other hand, the

Fig. 2 The variation of depletion width under bias for three different values of uncompensated defect densities. The insets indicate the charge distribution at the SCR and BC where the relevant diodes form and the current flows in corresponding direction. The reverse bias diminishes W_b by extending the SCR, whereas the forward bias reduces the strength of F and creates a back barrier at the BC



forward bias reduces the electric field and a double diode can show this state. In this case, the SCR is reduced by the forward biasing and the BC region can slightly increase. This is in agreement with all the conceptual studies in literature and the physical theory considered above [1, 14]. The reverse bias diminishes the W_b by extending the SCR, whereas the forward bias reduces the strength of F and creates a back barrier at the BC. Taking into account the effect of bias on the depletion widths and also the presence of the BC region, the JV characteristics of thin and ultrathin devices is represented in Fig. 3. Two CdTe devices with the thickness of 2.5 and 1 μm are simulated expected to have metallic Cu/Au BC. The rollover was diminished for the ultrathin film due to diminished back barrier by extended depletion width (W), to the BC of the ultrathin

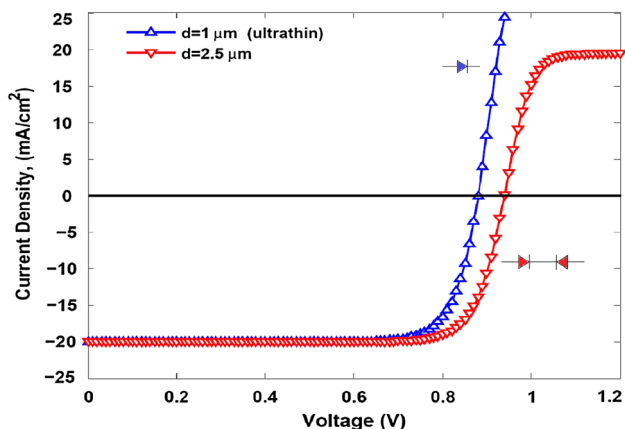
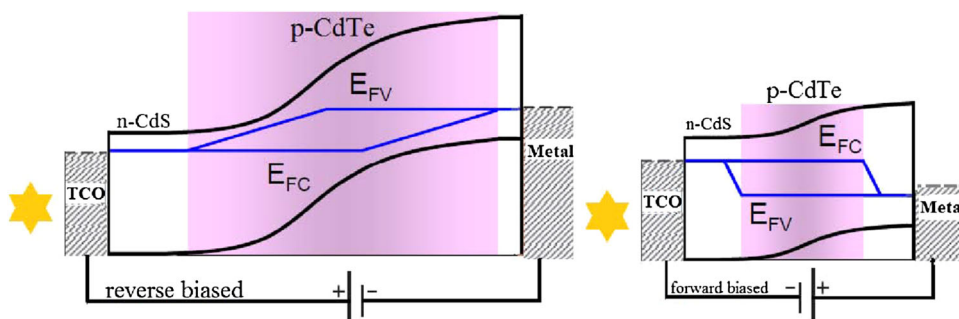


Fig. 3 The JV curves of thin and ultrathin film devices. The rollover is diminished for the ultrathin films with the thickness of about 1 μm . The diodes represent the junction and back barrier

layer. The rollover comes from the back barrier that impedes the carrier transport at the semiconductor/metal interface. This barrier acts as an opposite diode to the junction known as the origin of high series resistance in the degradation studies. The reduced CdTe will diminish this anomaly because in an ultrathin device, the carrier collection at the back region is covered by the electric field of the extended SCR. Thus, opposite diode in the back region is overcome by the main junction diode, and the carrier transport will not face any barrier at the BC. The result is in agreement with the analysis of Hadrich et al. [14] for the characteristics of thin/ultrathin CdTe devices with Cu/Au BCs. Therefore, while the rollover is a negative issue for the thin-film devices, it is not an effective phenomenon in ultrathin films. The practical reports in literature confirm the simulations in this regard with $d \leq 1 \mu\text{m}$ [15, 16] where the SCR and BC overlap and the rollover in the JV curves is diminished.

In order to obtain a clear insight into the carrier transport in ultrathin device, Fig. 4 represents the separation of the Fermi levels under reverse and forward biases. The remarked region displays the extended and reduced electric field supporting region for the RB and FB, respectively. So far, it is understood that the BC cannot effectively impede carrier transport at the back. Thus, for the rest of the simulations, we correctly assume that $W_{\text{tot}} \approx W(W_b \sim 0)$. Such assumptions will close our studies to the experimental analysis reported in literature and the other publications about the overlap between the depletion widths of the front and BC, and the fact that in ultrathin films, the SCR width is sufficient to explain the JV curves of the device.

Fig. 4 The redistribution of band diagram, electric field, depletion width and quasi-Fermi levels of the ultrathin films where the SCR width overlaps with the BC. The highlighted region in each biased device is the coverage region of the electric field



3.1 Degradation

The degradation of ultrathin films is a critical aspect of such devices because the thinner the CdTe layer, the faster is the accumulation of mobile ions (i.e. Cu^+ , Cl^- , S) at the junction. Since the BC and junction are closer in ultrathin films, the mobile ions will reach the junction in a shorter time under stress and both photo-conductivity and dark resistivity of the junction will increase. Finally, the degradation over time is appeared as a significant rollover in light/dark JV curves [17]. The accumulation of Cu^+ ions, which inter-diffuse from the BC to the junction, increases the deep/shallow acceptor densities in the depletion region. The increase in deep acceptor density will reduce the donor density and increase the recombination centres at the junction (in SCR). The same process can happen by the inter-diffusion of S from CdS into CdTe. Any variation in the density of donor/acceptor defects changes the Fermi level, recombination-generation rate and resistivity of the device (Fig. 5). The longer stressed devices show an irreversible degradation in electrical parameters.

Not only materials inter-diffusion, but also the humidity in the deposition or treatment ambient can be the resource of degradation when the device is operating under real condition. In this case, at the back surface, Oxygen complexes form as CdTeO_3 , TeO_2 or a mixture of both [18].

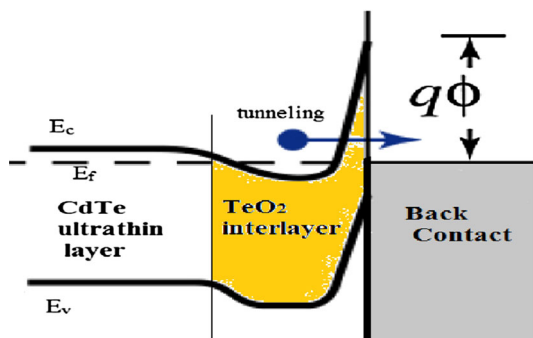


Fig. 5 Tunnelling mechanism enhanced by TeO_2 interlayer leading to enhanced carrier transport at the BC

The role of oxide interlayer is still under debate. For example, a very thin TeO_2 interlayer can contribute to enhance the carrier collection at the back region by tunnelling mechanism. Clearly, this transport is enhanced in ultrathin CdTe layers where the electric field is extended to the back region (Fig. 5).

The interlayer is not always a barrier for carrier transport and sometimes can assist the behaviour of the BC via tunnelling if the band gap at the interface with the metallic BC is large enough. The effect of stress on the properties of this thin interlayer has to be taken into account, and its collaboration in carrier transport and series resistance should be further considered. Oxygenation during CdS/CdTe deposition has a positive effect on the performance of the device if the concentration of oxygen (1–5 %) is optimized to obtain the proper grain size. However, as it was stated in Ref. [3], the oxidation of the back surface from the H_2O -containing environment can be a back barrier for the hole transport and cause rollover in the JV curves. The latter phenomena cannot be generalized as the oxygenation depends on the BC type. This process is reverse in Cu/Au metallic contacts. To recover the oxide insulating layer effect, etching and recontacting is suggested. Any etching by Br or Cr solutions applied to remove the oxide layers from CdTe surface is critical for ultrathin films as it may thin the film (remove the CdTe too much) and cause local shunting. To prevent the local shunting, self-healing method was suggested to create a barrier for the extra diffusion of those complexes and to remove the surface non-uniformities [16]. The few available ALT data in literature for the ultrathin film devices have not shown any significant degradation over time. Further analyses are required to track the behaviour of such devices. Nevertheless, the device stabilization through heating in dark, before back contacting, can protect against oxidation and extra Cu diffusion by the formation of Cu–Te complexes [3]. Though Cu^+ is considered to be a fast diffuser into CdTe ($D_n \sim 3 \times 10^{-12} \text{ cm}^2 \text{ s}^{-1}$), Cl treatment can accelerate this diffusion and formation of $\text{Cl}_S\text{--Cu}_{\text{Cd}}$ at the SCR. The Cu_{Cd} is formed across the CdTe ultrathin layer due to the presence of V_{Cd} or $\text{Cl}_S\text{--}V_{\text{Cd}}$. The

above discussions have been summarized in Table 1 representing the observed phenomena under different stress and operation conditions for (only) ultrathin CdTe films reported in the literature. Fortunately, light soaking the open-circuited device or heating in dark conditions can have reversible effect where the Cu^+ density is reduced (reduced acceptor density in CdS) and the cell is recovered [18]. Degradation of the device was reported with reduction in open-circuit voltage (V_{oc}), fill factor (FF) and short-circuit current density (J_{sc}), corresponding to the degradation of junction, BC and shunt resistance increase, respectively [20]. Most of the listed phenomena in Table 1 were attributed to the extra inter-diffusion of Cu^+ ions and the variation in the deep or shallow acceptor density in CdTe layer. In order to show the effect of electric field of the junction on the degradation rate of the device, Fig. 6 represents the schematic of band diagrams of short- and open-circuited devices under illumination, diffusion paths of ions/defects, complexes formation at the junction and BC. Clearly, the short-circuit condition will still keep the device under an electric field. On the other hand, the photovoltage induced from the illumination will try to reduce this field. However, the resultant of those biases will not be zero, and the total electric field is still able to impede the inter-diffusion of metallic atoms (Cu^+). Thus, the defect density is lower, and the degradation rate is slower in short-circuited device. On the other hand, the open-circuited device condition shows a reverse mechanism. The V_{oc} of the p-n junction will be diminished with the induced photo-voltage, and thus, the Cu^+ ions will diffuse faster into the CdTe layer almost without a barrier. The

degradation rate is higher in this case. The latter mechanism is addressed as recovery of the degraded devices. The strength of the electric field in short-circuited device has been indicated with the arrow while in the open-circuited device it was set as zero. All the degradation/recovery mechanisms are thermally activated due to the dependency of recrystallization on the temperature levels. Thus, annealing the devices under latter considered conditions can faster inter-/back-diffusion of the mobile ions.

3.2 Recovery

If we consider that the resultant of the electric fields in an open-circuited device under illumination (V_{oc} and photovoltage) can faster the diffusion of mobile ions into the CdTe layer and cause degradation, thus in the dark condition the reverse process occurs as recovery. In fact, the devices left in the dark condition while open-circuited have shown recovered performance. The same behaviours were observed by re-annealing in dark [21]. In literature, this mechanism is attributed to the reduced defect density (i.e. Cu^+ concentration) that are diffused back to the BC under the electric field at the SCR. Since, in the ultrathin device, the depletion width of the SCR is extended to the BC, the back-diffusion of the mobile ions under the extended electric field is rather probable. Figure 7 shows the analysis of the variation of JV curves at the reverse bias range. The distribution of uncompensated defects, N_{ads} , recombination lifetime, τ , and band bending, ϕ , was selected in a reasonable range for ultrathin CdTe films as reported in Ref. [5]. The defect density, E_t , was kept constant at 0.65 eV. It

Table 1 Reports on dominant phenomena under different operation conditions (only for ultrathin film PVs)

#	SC	OC	FB	RB	References
Light	Reduced deg.	Faster deg	Deg.	Slightly recovered	[4, 5, 19, 22]
Dark	Deg.	Recovery	Deg.	Recovery	[4, 5, 23]
Heat	–	Recovery	–	–	[3]

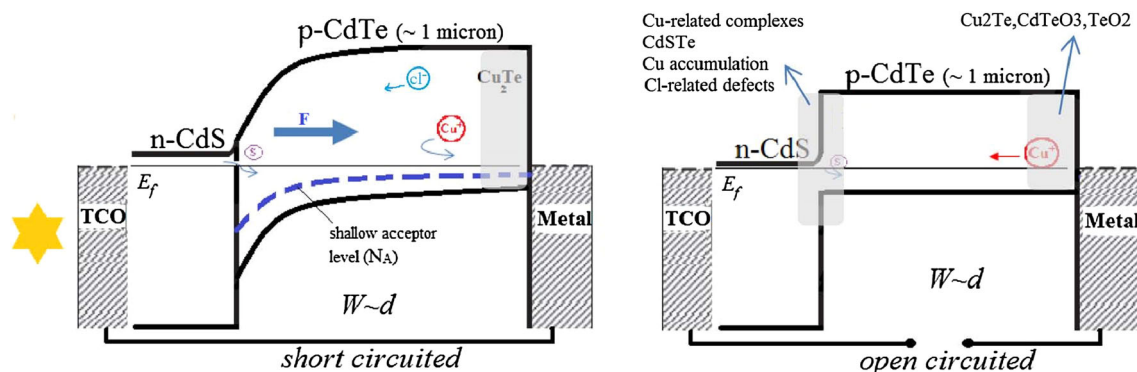


Fig. 6 The band diagrams of the short- and open-circuited devices under illumination. The inter-/back-diffusion of the defects (Cu^+ , S, Cl, etc.), electric field and the formation of complex thin interface layers have been addressed

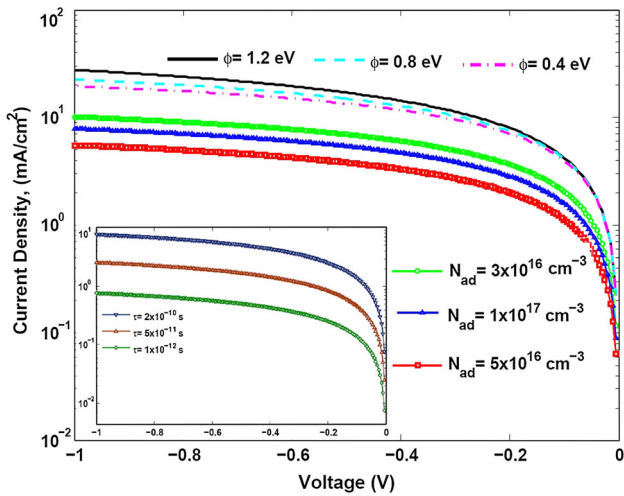


Fig. 7 The JV curves of the ultrathin film device at the reverse bias region. The different values of the parameters were selected in the reasonable range in order to avoid the overlap of the curves

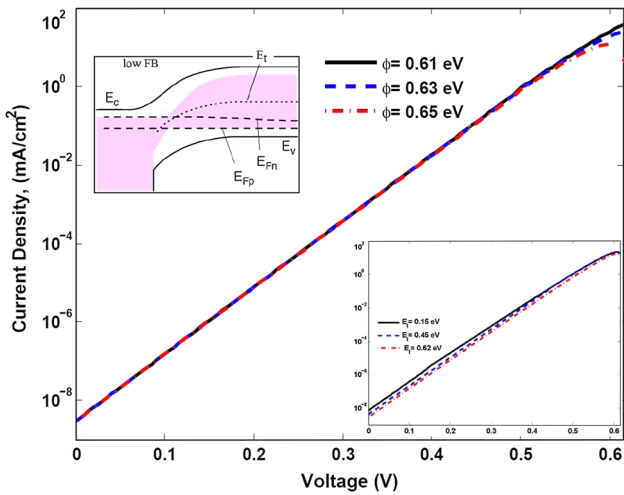
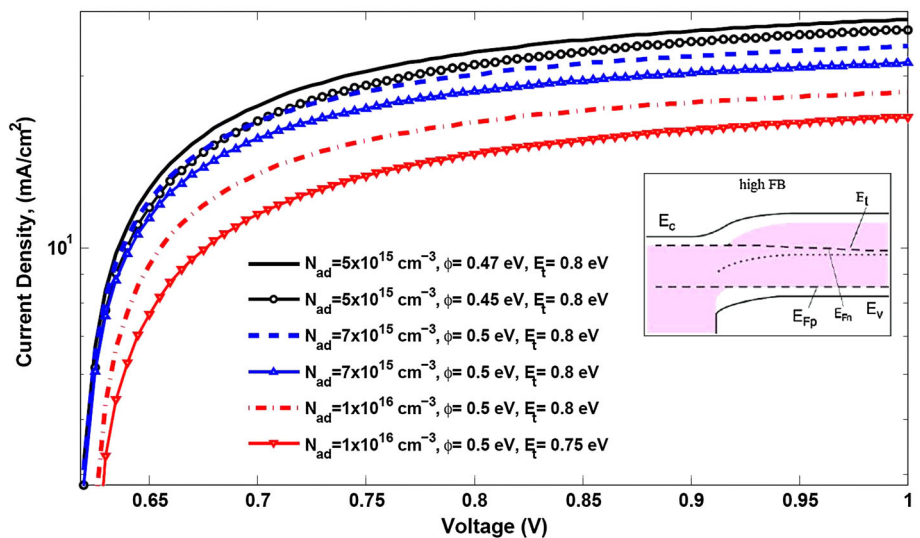


Fig. 8 The JV characteristics at lower forward biases for different values of ϕ and N_{ad} . The inset represents the effect of recombination lifetime (τ_n)

Fig. 9 The JV characteristics under forward-biased device ($V > 0.615$ V). Each two curve (solid and marked with the same colour) represents the variation of single parameters when the other two parameters are kept constant. The parameters have been justified in a reasonable range the way that the overlap between the curves is prevented

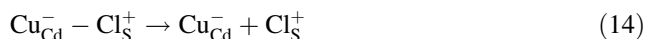
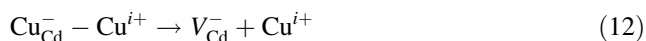


is assumed that the uncompensated defect density will reduce under the dark and open-circuited condition (Table 1). We calculated the JV curves for the case that N_{ad} reduced after storage for a short time. The variation of N_{ad} from 3×10^{16} to $1 \times 10^{17} \text{ cm}^{-3}$ could recover the current density while reduced band bending from $\phi = 1.2$ to 0.4 eV had a reverse effect on JV curve. The reduced band bending represents the increased defect density at SCR (reduced W). The closer valence and conduction bands (smaller ϕ) will put the generated carriers available to find each other and recombine. Moreover, smaller ϕ will shift the E_t closer to the minimum of conduction band and maximum of valence band where the recombination of Shockley–Read–Hall type is maximum. This is in consistency with the effect of recombination lifetime indicated in the inset of Fig. 7. The shorter lifetime leads to lower current density. The reduced Cu^+ concentration can longer the lifetime and cause recovery of JV curves. Remind that $\tau \propto 1/N_{ad}$. Note that in order to avoid the overlap of the curves, $E_t = 0.7$ eV was chosen when N_{ad} was changing. Practically talking, the recovery occurs when Cu impurities are reduced in the junction and bulk of the device. Therefore, after a while (days to months), the lower number of the defects will recover the depletion width, electric field. Clearly, the wider W will collect more generated carriers, and the current density is recovered again. This result is in consistency with the variation of W with N_{ad} . With a higher band bending, the recombination rate at the junction is reduced. The JV characteristics in forward range have been presented in Figs. 8 and 9 by Eqs. (4) and (5). The reason why we considered the different ranges of the forward bias separately is that each bias range is corresponding to a different defect (trap) level in the band gap. This is in agreement with the approach of double-diode model where two different ideality factors are attributed to the different voltage ranges. The latter reminds that two

different charge transport mechanisms are responsible in each voltage range. It is well known that the recombination at the SCR ($A \sim 2$) and diffusion at QNR ($1 < A < 2$) dominate the carrier transport. Ideality factor ≥ 2 represents that the Shockley–Read–Hall recombination is dominant by midgap states that is any decrease in their density would result in a reduction of the diode factor and improved cell performance. It is interesting that the diffusion current becomes important by about 0.62 V in the forward range. This indicates that in the ultrathin devices, the recombination current in SCR is less than the one in thin films until when the device goes under a stronger bias. For $V > 0.62$ V, the SCR is limited to a narrower distance close to junction where the recombination mechanism (with $E_t = 0.72$ eV) can overcome the transport. Note that, the observed JV characteristics were obtained in terms of recombination in the SCR without involving the thermionic emission. For a better understanding, three different value of ϕ and E_t were examined in forward bias range of $0 < V < 0.615$ V. The deviation of the curves is started when $V \sim 0.6$ V while varying the trap level manifests itself at the lower voltages (inset of Fig. 8). As we noted before, the lower band bending reduces the current density (due to higher recombination at the SCR). Similarly, the closer trap level (E_t) to the midgap (0.75 eV) damages the current density. The Sah–Noyce–Shockley theory well describes the JV characteristics of both the forward and reverse currents of CdS/CdTe solar cells depending on the uncompensated defect density, carrier recombination lifetimes and other parameters of the CdTe layer, which represent a physical meaning rather than the conventional single or double-diode models with an engineering background. The JV curves at high FB represent the R_s which is a parameter of the all device mostly from BC issues [24]. The behaviours of the ultrathin device at higher forward biases ($V > 0.615$ V) are rather consistent with the JV characteristics of the thin-film devices. The different values of parameters have been used to simulate the recovery mechanism in CdTe layer. Forward biasing can reduce the width of SCR and make significant the role of $W \propto 1/N_{ad}$. For each two curves (solid and marked with the same colour), one of the parameters is varied and the two others are kept constant. We tried to keep the simulation closer to reality by selecting the value of the parameters in the range of the practical reported data in literature and desirable for the CdTe device. All the above discussions remind the role of metallic contacting in controlling the defect density (deep/shallow acceptor/donor states). Unfortunately, there are very few investigations in this matter. Paudel et al. have reported that the $\text{MoO}_{3-x}/\text{Au}$ BC on ultrathin CdTe can be replaced by Cu, but the performance is reduced. The degradation behaviours of those devices under stress were not presented [25]. The inter-diffused Cu^+ under stress is

accumulated at the CdS/CdTe interface. In addition to mobile Cu^+ ions, Cl atoms are also diffused into CdTe (through post-growth treatment/annealing) and are accumulated at the junction. Moreover, Cl can accelerate the Cu diffusion rate thus back contacting and CdCl_2 post-growth treatment/annealing should be reoptimized for ultrathin devices. On the other hand, heating the device before stressing can stabilize the performance. This mechanism was attributed to the formation of a thin Cu_{2-x}Te layer at the interface of CdTe/metal. The higher density of favourable Cu_{2-x}Te lowers the Cu^+ diffusion rate into CdTe, which, in turn, reduces the degradation rate under stress [3]. Therefore, the formation of Cu_{2-x}Te complexes is favourable to the recovery of the film. However, the effect of this thin layer at the BC needs to be studied specifically for the ultrathin films where the back barrier is disappeared by the overlap of the depletion width. In contrary to the favourable effect of Cu_2Te layer, it was also detected that Cu_2Te can be a source of Cu extra inter-diffusion into the junction [18]. In all the curves presented, the effect of carrier recombination lifetime at E_t is significant. In practice, the carrier lifetime is usually much smaller “near the back contact”. In fact, time-resolved photoluminescence as a function of depth can give experimental values of the space-dependent lifetimes. Again, Cu can easily diffuse to the absorber layer from the back contact in shorter devices and eventually acts as recombination centres. The interface effects are more prominent in shorter devices. Shorter carrier lifetimes in thinner devices result in leakage current increment and reduced photocurrent, which, in turn, lowers the V_{oc} and FF. Ultrathin solar cells with small grains are prone to form shunt paths (reduction of R_p) and shorter the carrier lifetime [26]. Kabir et al. have analysed the role of holes in carrier transport of the ultrathin films. The photo-generated electrons quickly move towards CdS layer, whereas holes have to travel a longer distance in the CdTe layer. Therefore, the charge collection efficiency is mainly controlled by the hole transport [27]. We have also taken this into account introducing the p and N_{ad} in the theory section of this work. Gupta et al. have developed an efficient deposition technique to increase the grain size and to ensure high-quality CdTe films [16]. Grain growth and recrystallization can reduce recombination paths and thus enhance the carrier lifetime. For the sake of completion, we note that the hot spot runaway will be one of the irreversible issues especially in ultrathin films where physically removing the shunted area could be the only solution [28]. The inset of Figs. 8 and 9 schematically shows the position of the recombination level for two different forward bias regions. For small forward biases, the efficient recombination region is very narrow, and E_t generates only a small recombination current. At higher forward bias, however,

the region of efficient recombination is much wider, and the total recombination current is higher. The variation of depletion width is significant in each case. The complex formation across the CdTe layer or at the interfaces might be well analysed for the ultrathin films. Formation of $\text{Cl}_S\text{-Cu}_{\text{Cd}}$ complexes keeps the Cu^+ immobile. This prevents the Cu atoms to play the role of deep defects in the CdTe and reduce the performance as well. In recovery mechanism, the back-diffusion of the Cu^+ ions reduces the density of deep defects across the CdTe layer. Note that the formation of Cu-related complexes is accelerated by Cl concentration around the junction. The increase in the acceptor density (increased Cu atoms) can reduce the donor density in CdS (or at the SCR), and thus, the conductivity of the layer is reduced (increase the series resistance). The photoluminescence study indicated that the dissociation of those complexes under reverse bias and re-annealing, can partially recover the performance [21, 29]. From Fig. 6, it is understood that the degradation under bias can be recovered by opposite biasing the device. Clearly, the light soaking before back contacting can stabilize the device. The reason is that the concentrations of complexes with Cd vacancies are reduced and lead to lower defect densities of the following types:



The above counterbalance shows also the variation in the shallow acceptor or deep donor defect densities under stress. Despite the above considerations, Krasikov et al. [30] have theoretically shown the formation of $V_{\text{Cd}}^- + \text{Cu}^{i+}$ defect. Saying that Cu^+ is readily replaced with $\text{Cu}_{\text{Cd}}^- + \text{Cu}^{i+}$ is unlikely because it transforms into the Cu_{Cd} in CdTe. This is why the Cu_i is found in the entire of CdTe thickness as it is the only mobile specie at room temperature. Grecu et al. [29] have investigated that the device finished with Cu-free contacts (Ag) can show reversible degradation by re-annealing after stressing. Further investigations are required to determine the advantage of Cu-free contacts and their degradation/recovery rate by acceleration life testing. The interface layer of CuTe could be also a resource of Cu for the ultrathin CdTe film. The optimized layer of Cu-Te can be a barrier for the Cu to the CdTe layer. The concern is when this layer prevents Cu inter-diffusion into CdTe that can increase the conductivity of this layer. We might remind that our approach does not take into account the diffusion of the defective particles through grain boundaries but it assumes that the CdTe layer is a slab. This is a valid assumption as in the ultrathin films,

and the grain size of $\geq 1 \mu\text{m}$ is comparable with the CdTe thickness. The strong electric field in this structure could be sufficient to accelerate the ions across the CdTe layer through the grains interior. In above investigations, we have neglected the role of metal diffusion through grain boundaries which are assumed to be completely passivated. This can be realized by an optimized chlorine treatment or improved deposition and post-growth annealing the film. This assumption enabled us to study the role of other mechanisms, separately. This is because the other instability phenomena are usually hidden behind the metal diffusion into grain boundaries and a clear understanding of these phenomena have not been well studied yet. In this case, we assumed that the grain boundaries are well passivated, and the metallic ions are not easily diffusion towards the junction under stress conditions.

4 Summary

Ultrathin film devices based on CdTe have been theoretically analysed in order to obtain an insight into the physics of such particular devices. Reducing the CdTe thickness to $< 1 \mu\text{m}$ is essential in order to: (1) reduce the price of the device, (2) reduce the usage of rare Te and hazardous Cd components, (3) reduce the fabrication time in large production lines and (4) reduce the toxic components. We have discussed the degradation and recovery of JV characteristics and calculated the variations under reverse and forward bias ranges. Several physical parameters such as uncompensated defect density, carrier recombination lifetime and band bending at the junction of CdS/CdTe were taken into consideration using the Sah-Noyce-Shockley theory for generation-recombination in the SCR. The depletion width was simulated for each biasing profile for several defect densities. The rollover in the JV curve was shown to be disappeared for the ultrathin devices because of the extended electric field to the BC. This work provides a physical analysis based on the band diagrams and the experimental reports in literature suggesting that the growth and deposition conditions need to be reoptimized for ultrathin devices since the re-growth and inter-diffusion of the device components seem to accelerate with thinner CdTe layer. The recovery of the ultrathin solar cell happens when the mobile Cu^+ ions are diffused back to the BC, and the concentration of the acceptor density (deep/shallow) is reduced across the device especially at the junction. We note that in this work, we have assumed that CdTe layer is like a slab and the defects diffuse from the BC to the junction through bulk of the grains. The inter-diffusion through the grain boundaries can be modelled by the weak diode or shunting pathways approaches. The proper bias, illumination and heating conditions can faster the recovery

process as abstracted in Table 1. The Effect of uncompensated acceptor concentration, band bending and carrier lifetime on the JV characteristics indicates that, in fact, inter-diffusion of the materials and/or accumulation of the ions at the junction (SCR) or BC can cause degradation. The reverse process can recover the electrical parameters. All the changes in JV curves were due to variation in electric field that is responsible for the carrier transport and carrier collection.

References

- V.G. Karpov, M.L.C. Cooray, D. Shvydka, *Appl. Phys. Lett.* **89**(16), 163518 (2006)
- L.A. Kosyachenko, T. Toyama, *Sol. Energy Mater. Sol. Cells* **120**, 512–520 (2014)
- I.V. Fisher, K.D. Dobson, G. Hodes, D. Cahen, *Adv. Funct. Mater.* **13**, 289–299 (2003)
- N. Paudel, K. Wieland, M. Young, S. Asher, A. Compaan, *Prog. Photovolt. Res. Appl.* **22**, 107–114 (2014)
- V. Plotnikov, X. Liu, N. Paudel, K. Wieland, A. Compaan, *Thin Solid Films* **519**, 7134–7137 (2011)
- S. Hegedus, D. Desai, D. Ryan, B. McCandless, in *Proceedings of 31th IEEE Conference*, (2005), pp. 319–322
- L.A. Kosyachenko, O. Maslyanchuk, V. Sklyarchuk, *J. Appl. Phys.* **101**(1), 013704 (2007)
- D. Regesch, L. Gutay, J. Larsen, D. Tanaka, Y. Aida, S. Siebentritt, *Appl. Phys. Lett.* **101**, 112108 (2012)
- V. Plotnikov, C. Carter, N. Paudel, A. Compaan, in *Proceedings of 39th IEEE Conference*, (2013), pp. 0405–0408
- N.E. Gorji, *Phys. B* **431**, 44–48 (2013)
- L.A. Kosyachenko, O.L. Maslyanchuk, V.M. Sklyarchuk, *Sol Energy Mater. Sol. Cells* **82**, 65–73 (2004)
- C. Sah, R. Noyce, W. Shockley, *Proc. IRE* **46**, 1228–1243 (1957)
- L.A. Kosyachenko, X. Mathew, V.V. Motushchuk, V.M. Sklyarchuk, *Sol. Energy* **80**, 148–155 (2006)
- M. Hadrich, C. Heisler, U. Reislohner, C. Kraft, H. Metzner, *Thin Solid Films* **519**, 7156–7159 (2011)
- N.R. Paudel, K.A. Wieland, A.D. Compaan, *Sol. Energy Mater. Sol. Cells* **105**, 109–112 (2012)
- A. Gupta, V. Parikh, A.D. Compaan, *Sol. Energy Mater. Sol. Cells* **90**, 2263–2271 (2006)
- T.J. McMahon, A. L. Fahrenbruch, in *Proceedings of 28th IEEE Conference* (Anchorage, 2000) pp. 539–542
- K.D. Dobson, I. Visoly-Fisher, G. Hodes, D. Cahen, *Sol. Energy Mater. Sol. Cells* **62**, 295–325 (2000)
- D.T. Morgan, in *M.Sc. Thesis: An Investigation into Degradation of CdTe Solar Cells* (Colorado School of Mines, Colorado)
- N.E. Gorji, *Appl. Phys. A*, **116**(3), 1347–1352 (2014)
- D. Grecu, A.D. Compaan, D. Young, U. Jayamaha, D.H. Rose, *J. Appl. Phys.* **88**(5), 2490 (2000)
- D.S. Albin, J.A. del Cueto, in *IEEE Conference on Reliability Physics. (IRPS)* (Anaheim, 2010) pp. 318–322
- T.D. Dzhafarov, S.S. Yesilkaya, N.Y. Canli, M. Caliskan, *Sol. Energy Mater. Sol. Cells* **85**, 371–383 (2005)
- I.M. Dharmadasa, *Advances in Thin Film Solar Cells* (Pan Stanford Publishing, Berkeley, 2013)
- N.R. Paudel, A. Compaan, Y. Yan, *J. Electron. Mater.* **15** (2014), 43(8), pp. 2783–2787
- S. Mahmood, M.Z. Kabir, O. Tousignant, J. Greenspan, *IEEE Trans. Nuc. Sci.* **59**(3), 597 (2012)
- S.M. Arnab, M.Z. Kabir, *J. Vac. Sci. Technol. A* **31**(6), 061201 (2013)
- N.E. Gorji, *IEEE Trans. Device Mater. Reliab.* **14**(4), 983–988 (2014)
- D. Grecu, A.D. Compaan, *Appl. Phys. Lett.* **75**(3), 361 (1999)
- D. Krasikov, A. Knizhnik, B. Potapkin, S. Selezneva, T. Sommerer, *Thin Solid Films* **535**, 322–325 (2013)